

A SIMPLE MAXIMUM POWER POINT TRACKER UTILIZING THE RIPPLE CORRELATION CONTROL TECHNIQUE

Mark Savenkov¹ & Rowan Gobey¹

¹Student at the School of Electrical & Computer Engineering
RMIT University, Melbourne, Australia

Correspondence to: M. Savenkov (savenkov@gmail.com)

ABSTRACT

Significant gains in photovoltaic system efficiency can be realized by way of a maximum power point tracker (MPPT). This form of power converter ensures a photovoltaic module runs at its highest level of efficiency by keeping its operating point at the knee of the photovoltaic current-voltage curve. The authors have developed and fabricated a low cost MPPT that utilizes the ripple correlation control (RCC) technique. RCC is reasonably well grounded within the literature and suited to a variety of photovoltaic applications.

INTRODUCTION

A photovoltaic panel has an output characteristic dependent on conditions such as illumination intensity and temperature. Each output characteristics has a unique maximum power point (MPP) where the current-voltage product is greatest. The purpose of a maximum power point tracker (MPPT) is to ensure a photovoltaic panel runs at its highest level of efficiency by keeping it operating at the MPP, regardless of changes in external conditions. An MPPT typically consists of a step-up or step-down DC-DC converter and some form of duty-cycle control circuit.

This paper describes a low cost MPPT that utilizes the ripple correlation control (RCC) technique and is suited to a variety of applications, such as standalone photovoltaic power supplies, solar powered cars, or even student laboratory experiments. It should be noted that this paper is based on an undergraduate (final year Engineering) project and the control circuit presented here is an extension of a design originally proposed by Lim & Hamill (2000, 2001).

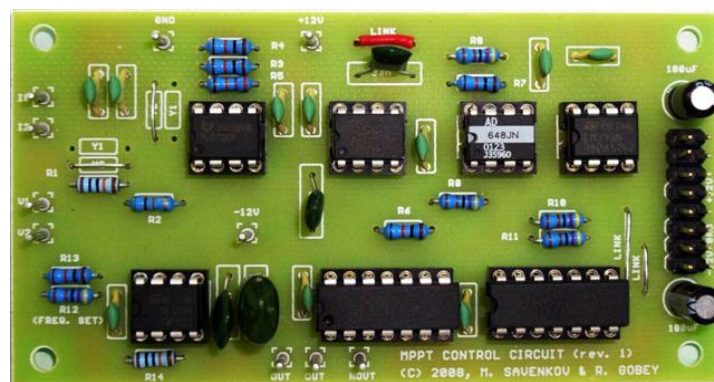


Fig. 1: Prototype MPPT control circuit

The paper is organized as follows. A short literature review is provided in the following section, concentrating on MPPT control techniques that can be realized in a low cost, and preferably analog form. In the next section a control circuit is described in detail, including its operation and implementation. Then results of a PSpice simulation are reported, with particular emphasis on the process of MPP capture. Lastly, simulation results are briefly compared with experimental results using a hardware prototype (pictured in Figure 1).

LITERATURE REVIEW

Upwards of 170 papers and nineteen distinct MPPT control techniques exist within the literature; separating each technique are differences in complexity, cost, tracking speed, and other characteristics (Esrām *et al.* 2006, Esrām & Chapman 2007). A limited amount of papers describing low cost analog control circuits will be discussed here.

Fixed reference voltage

Maheshappa *et al.* (1998) and Huang (2000) develop low cost fixed reference voltage MPPT control circuits. In each of these cases, the array voltage is compared with a reference voltage corresponding to an array voltage at a given maximum power point. A major drawback of this technique is its need for manual re-adjustment as atmospheric conditions change.

Hill climbing

Most MPPT controller literature is devoted to the ‘hill climbing’ (or ‘perturb and observe’) approach (where the ‘hill’ represents a unique photovoltaic power versus voltage or current curve). In this case, the array voltage is perturbed (increased or decreased), the change in power noted, and the direction of the next perturbation is implemented accordingly. There are usually four modes of steady state operation. A general algorithm describing the process is given in Esrām & Chapman (2007).

An analog (incorporating discreet digital components) circuit of this kind has been developed by Kim *et al.* (1996); though, it should be emphasized that digital (microcontroller based) hill climbing control circuits are much more popular than their analog counterparts—examples of these include Jiang *et al.* (2005), Tokushima *et al.* (2006), and several others. Apart from being difficult to realize in an inexpensive analog form, the hill climbing technique is criticized for being sensitive to abrupt changes in atmospheric conditions (see for example Esrām & Chapman 2007).

Voltage maximizing

Lower cost variations of the hill climbing technique sometimes make use of a two mode repeated perturbation (or ‘voltage maximizing’) approach. De Cesare *et al.* (2006) develop a circuit of this kind where the direction of load voltage is sensed, duty cycle is then varied in the same direction (e.g. in the positive direction), and then varied again if the sign of voltage remains unchanged (i.e. positive). The process repeats itself until the load voltage changes direction. This particular approach is only suitable for resistive loads, and is generally less efficient than a traditional hill climbing implementation;

however, it is capable of withstanding demanding atmospheric conditions (De Cesare *et al.* 2006).

Ripple correlation control

Ripple correlation control (RCC) was first proposed by Midya *et al.* (1996) for MPPT and motor efficiency optimization purposes. Inexpensive and robust controllers utilizing an analog RCC technique have also been developed by Esham *et al.* (2007), Il-Song & Myung-Joong (2004) and Lim & Hamill (2000, 2001). RCC makes use of converter ripple as an alternate source of perturbation. The maximum power point is usually located by correlating the derivative of the array power with the voltage or current ripple waveform. For example, the product of power and voltage derivatives with respect to time is zero at the MPP, but yields a positive and negative sign when the operating point is to the left or right (respectively) of the MPP (Esham & Chapman 2007, Kimball & Krein 2007, Midya *et al.* 1996). As Midya *et al.* (1996:1710) note, a major benefit of RCC is that it ‘keeps [DC–DC] converter operation at the optimum point’ while avoiding the ‘inconvenient, slow, and fundamentally sub-optimal’ perturbation process described in previous sections.

CONTROLLER OPERATION

In this work the authors are adopting a step-down DC-DC converter and analog ripple correlation control (RCC) scheme with voltage and current sensing capabilities. Converter and controller block diagrams are given in Figures 2 & 3—the controller makes use of a hysteresis variant of RCC and is based predominantly on work by Lim & Hamill (2000, 2001). While a step-down converter has been chosen for this project, a step-up converter could have easily been substituted in its place.

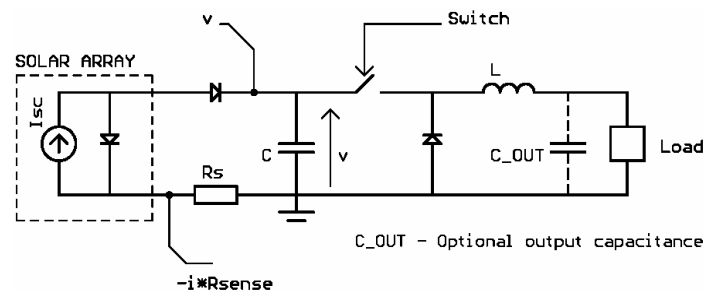
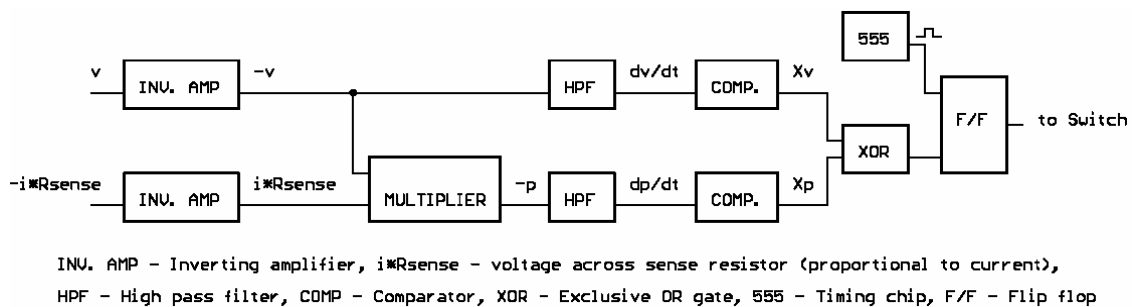


Fig. 2: Step-down converter



INV. AMP - Inverting amplifier, $i \cdot R_{sense}$ - voltage across sense resistor (proportional to current), HPF - High pass filter, COMP - Comparator, XOR - Exclusive OR gate, 555 - Timing chip, F/F - Flip flop

Fig. 3: Proposed controller block diagram

Figure 3 is described more fully by Figure 4. The controller senses array voltage and current; for current measurement a very small ($\sim 0.5 \Omega$) resistance is used to minimize excess power dissipation. These measured values are both inverted (and attenuated or amplified) before being fed to an analog multiplier to extract a measurement of array power. The measured power and voltage waveforms are approximately differentiated using high pass filters and then compared with respect to a ground reference; the comparator output pins include a pull-up resistor to a 12 V rail, which results in a comparator output of 12 V (or logic 1) for a positive voltage or power differential and 0 V (or logic 0) for a negative voltage or power differential. Since each comparator has only binary states there are four steady-state modes of operation—these modes are evaluated by an exclusive-OR gate and then sampled by a D-type flip-flop clocked at a constant frequency. The flip-flop output provides a suitable signal to drive a DC-DC converter switch.

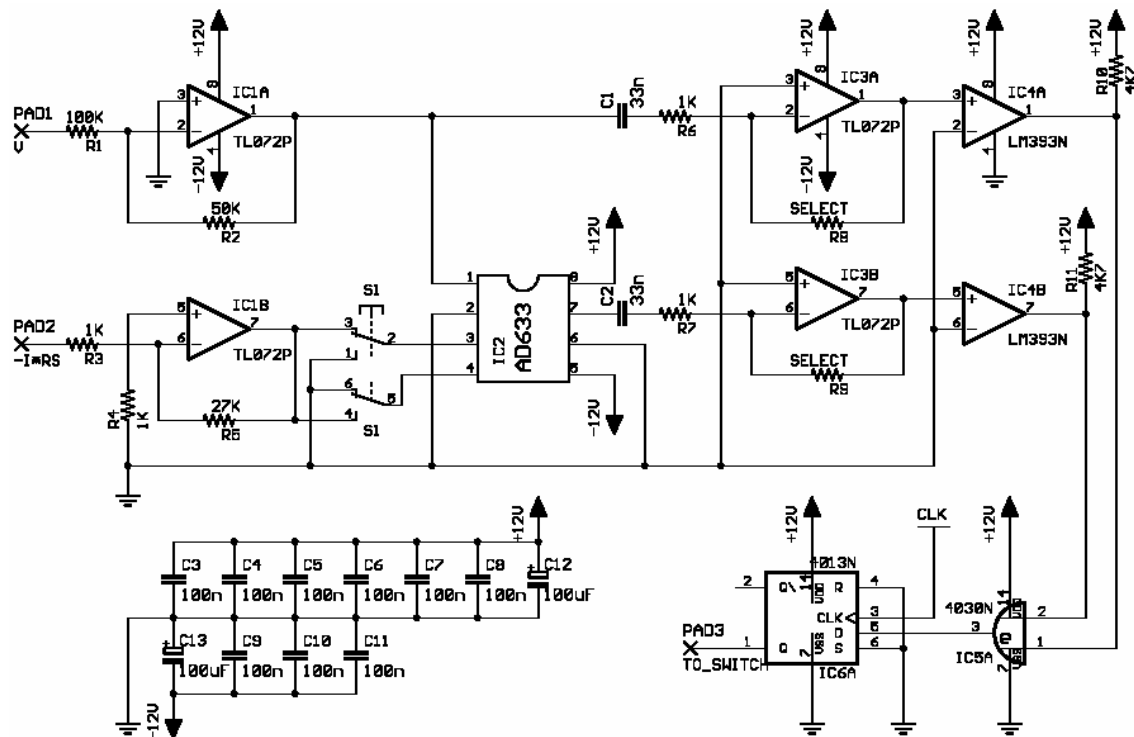


Fig. 4: Proposed controller circuit diagram

A summary of the controller operation is given in Table 1 (adapted from Lim & Hamill 2000, 2001). When each comparator state is the same, that is, when both the measured power and the measured voltage are either increasing or decreasing—and consequently the array voltage is less than the voltage at maximum power—the converter switch is open and the voltage seen by the converter increases. The opposite is true when the comparator outputs are not-equivalent to one another, that is, when either the measured voltage increases while the measured power decreases, or when the measured power increases while the measured voltage decreases—and consequently the array voltage is greater than the voltage at the maximum power point—for these cases the converter switch is closed and the voltage seen by the converter decreases. In practice, the voltage seen by the converter should oscillate around its optimum value.

Tab. 1: Summary of controller operation (see also Lim & Hamill 2000, 2001)

state		dp/dt		dv/dt		Comparator output		
						Xp	Xv	F/F
v	$\leq V_{mpp}$	> 0	> 0	1	1	0	charges	increases
v	$\leq V_{mpp}$	≤ 0	≤ 0	0	0	0	charges	increases
v	$> V_{mpp}$	> 0	≤ 0	1	0	1	discharges	decreases
v	$> V_{mpp}$	≤ 0	> 0	0	1	1	discharges	decreases

Before proceeding it would be wise to make a few more remarks regarding Figure 4. One of the design objectives for this circuit was to use a low parts count, another objective was to use a solitary bi-polar (-/+12 V) power supply. For these reasons the authors chose dual op-amps, a dual comparator, and CMOS gates.

The dual comparator (LM393) is powered by GND / +12 V rails. In its present configuration the LM393 will accept a negative voltage down to -0.3 V (and slightly beyond) before defaulting to a 0 V output. This means that the high pass filter (inverting differentiator) feedback resistors R8 and R9 should be chosen carefully to ensure that the comparator non-inverting inputs are (preferably) seeing a voltage within a range of -0.3 thru to +0.3 volts. For small R8 and R9 values it would be beneficial to replace IC3 with an op-amp that has a lower offset voltage (such as an AD648). Alternatively, R8 and R9 can be given a large value (100 K or more) however this might necessitate a voltage divider (200 K in series followed by a 4.7 K shunt) between the high pass filter and the comparator stages.

Included in the circuit diagram is a switch (S1). This switch allows the operator to select between an inverting or non-inverting multiplier input; in other words, for switching between positive and negative current sense. Not included in the circuit diagram, but probably beneficial, are input and output trim-pots to adjust for various input voltage levels (to model different sizes of PV arrays) and DC-DC switching voltage levels. Also lacking in the circuit diagram, but included in the prototype is a fixed (clocking) square wave oscillator (~12 kHz, 0 to 12 V) built from a 555 timer. This oscillator is used to clock the flip-flop, and set the system switching frequency.

CONTROLLER SIMULATION

The dynamic response of the controller has been tested using PSpice simulation. A solar array was modeled using a current source and string of diodes, while a DC-DC converter was modeled using ideal diodes, $C = 500 \mu\text{F}$, $L = 3 \text{ mH}$, and loaded with a constant voltage sink. The PSpice system was clocked at 10 kHz.

Variations in the solar array characteristics were created by switching between diode strings (simulating a change in temperature) and switching between short circuit current settings (simulating a change in solar illumination). For example, Figure 5 depicts an abrupt change in simulated temperature, and Figure 6 depicts an abrupt change in simulated illumination. In both cases array voltage and power rapidly track, and capture, an optimum value. The right hand graphs of Figure 5 and 6 are particularly revealing, as they illustrate the way in which the controller navigates the non-linear voltage-power curve ('hill') to its maxima. In Figures 5 and 6 the value of P/P_{max} (ideally 1) is provided

for a single case only. To establish P_{\max} the control circuit was disabled and the converter duty ratio was varied manually.

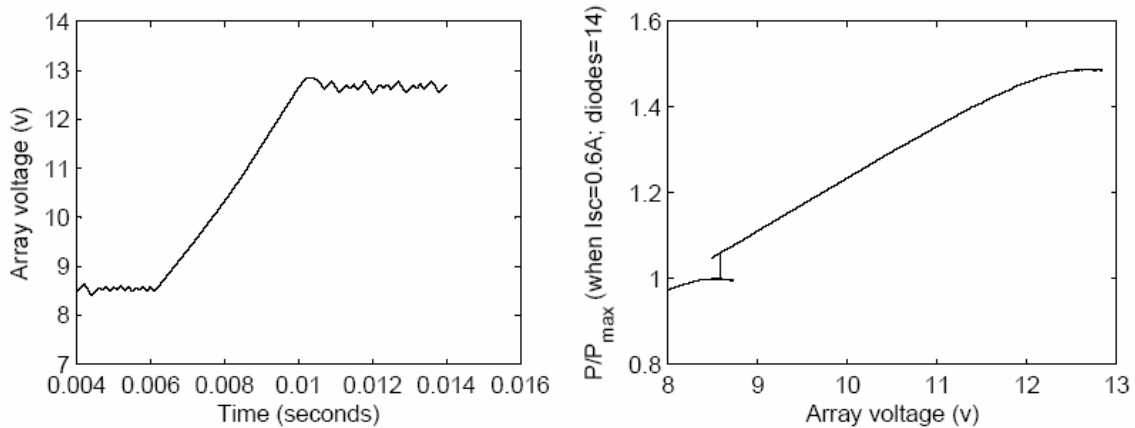


Fig. 5: PSpice simulation; number of array diodes switched from 14 to 20 while $I_{sc} = 0.6$ A; (left) array voltage vs. time, (right) corresponding power vs. voltage response

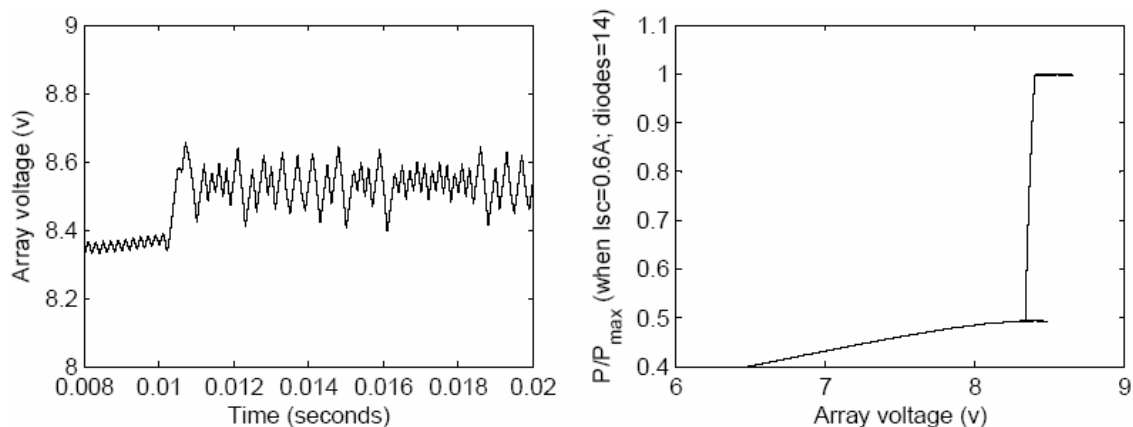


Fig. 6: PSpice simulation; I_{sc} switched from 0.3 A to 0.6 A while array diodes = 14; (left) array voltage vs. time, (right) corresponding power vs. voltage response

EXPERIMENTAL RESULTS

The authors have fabricated an MPPT control circuit (see Figure 1). In order to evaluate the performance of the MPPT control circuit a DC-DC converter and simulated solar array were also constructed. The experimental DC-DC converter was designed to closely replicate its associated PSpice model, with parameter values: $C = 470$ μF , $L = 3.2$ mH. The simulated solar array consisted of a current source and two diode strings (high current, ultra fast recovery), with the ability to switch between these strings. Also included in the simulated array was a small fan to regulate the temperature of the diodes. This hardware system was clocked at approximately 12 kHz using a 555 timer built into the control circuit.

An experimental system dynamic response example is provided in Figure 7. In this case the short circuit current was set at approximately 0.6 A while the diode string was switched from 9 to 14 (simulating a radical change in temperature). The experimental

voltage-time and voltage-power curves are in general agreement with results of PSpice simulation.

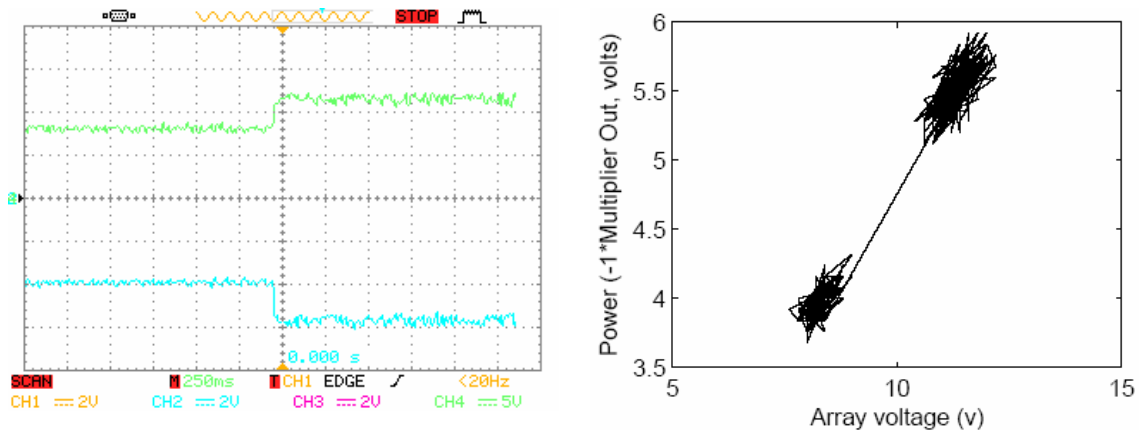


Fig. 7: Experimental observation; number of array diodes switched from 9 to 14 while $I_{sc} \approx 0.6$ A; (left) array voltage, green/upper, and AD633 multiplier output, blue/lower, over time, (right) corresponding power vs. voltage response

The experimental MPPT efficiency (P/P_{max}) was measured for a limited amount of static scenarios. Once again, to establish P_{max} the control circuit was disabled and the converter duty ratio was varied manually. In each case the efficiency—neglecting the parasitic load—was close to unity, and not less than 0.95. Overall the hardware control circuit prototype functioned in much the same manner as predicted by PSpice.

CONCLUSION

A simple and inexpensive maximum power point tracker, utilizing the ripple correlation control technique, has been developed and constructed. The MPPT controller is based on a design by Lim & Hamill (2000, 2001) and shares the same operating principles; however, this particular embodiment is physically smaller (having a reduced parts count) and functions on a solitary bi-polar power supply. It has been shown that when changes in temperature or solar illumination occur the controller rapidly shifts the system operating point to an updated MPP. The controller has a convergence rate in the order of milliseconds, and a high level of tracking effectiveness.

ACKNOWLEDGEMENTS

The authors would like to thank Dr. Y. H. (Bruce) Lim and Mr. David Latter for their insights and encouragement.

REFERENCES

De Cesare, G, Caputo, D & Nascetti, A 2006, 'Maximum power point tracker for portable photovoltaic systems with resistive-like load', *Solar Energy*, vol. 80, no. 8, pp. 982-988.

- Esrām, T & Chapman, PL 2007, 'Comparison of photovoltaic array maximum power point tracking techniques', *IEEE Transactions on Energy Conversion*, vol. 22, no. 2, pp. 439-449.
- Esrām, T, Kimball, JW, Krein, PT, Chapman, PL & Midya, P 2006, 'Dynamic maximum power point tracking of photovoltaic arrays using ripple correlation control', *IEEE Transactions on Power Electronics*, vol. 21, no. 5, pp. 1282-1291
- Huang, CC 2000, 'Hardware development of MPPT for solar powered model vehicle', undergraduate dissertation, School of Electrical and Computer Engineering, Curtin University (Perth).
- Il-Song, K & Myung-Joong, Y 2004, 'Single-loop maximum power point tracker with fast settling time', IEEE Industrial Electronics Society (30th Annual Conference), pp. 862-866.
- Jiang, J, Huang, T, Hsiao, Y & Chen, C 2005, 'Maximum power tracking for photovoltaic power systems', *Tamkang Journal of Science and Engineering*, vol. 8, no. 2, pp. 147-153.
- Kim, Y, Jo, H & Kim, D 1996, 'A new peak power tracker for cost-effective photovoltaic power system', Proceedings of the 31st Intersociety Energy Conversion Conference, pp. 1673-1678.
- Kimball, J & Krein, P 2007, 'Digital ripple correlation control for photovoltaic applications', Proceedings of the IEEE Power Electronics Specialists Conferences (PESC), pp. 1690-1694.
- Lim, YH & Hamill, DC 2000, 'Simple maximum power point tracker for photovoltaic arrays', *IEE Electronic Letters*, vol. 36, no. 11, pp. 997-999.
- Lim, YH & Hamill, DC 2001, 'Synthesis, simulation and experimental verification of a maximum power point tracker from nonlinear dynamics', 32nd Annual IEEE Power Electronics Specialists Conference, pp. 199-204.
- Maheshappa, H, Nagaraju, J & Krishna-Murthy, M 1998, 'An improved maximum power point tracker using a step up converter with current locked loop', *Renewable Energy*, vol. 13, no. 2, pp. 195-201.
- Midya, P, Krein, PT, Turnbull, RJ, Reppa, R & Kimball, J 1996, 'Dynamic maximum power point tracker for photovoltaic applications', 27th Annual IEEE Power Electronics Specialists Conference, pp. 1710-1716.
- Tokushima, D, Uchida, M, Kanbei, S, Ishikawa, H & Naitoh, H 2006, 'A new MPPT control for photovoltaic panels by instantaneous maximum power point tracking', *Electrical Engineering in Japan*, vol. 157, no. 3, pp. 73-80.